An Automated Evaluation Method of Tool Surface Condition in Composites Manufacturing Using Machine Learning and Sparse Sensing

Caleb Schoenholz; Shuangshan Li; Kyle Bainbridge; Vy Huynh; Alex Gray; Xu Chen; Navid Zobeiry

AN AUTOMATED EVALUATION METHOD OF TOOL SURFACE CONDITION IN COMPOSITES MANUFACTURING USING MACHINE LEARNING AND SPARSE SENSING

Caleb Schoenholz[1], Shuangshan Li[1,2], Kyle Bainbridge[1], Vy Huynh[1], Alex Gray[1], Xu Chen[3], Navid Zobeiry[1]
[1]Materials Science & Engineering Department, University of Washington
302 Roberts Hall, Box 352120
Seattle, WA 98195-2120, USA.
[2]Applied Mathematics Department, University of Washington
201 Lewis Hall, Box 353925
Seattle, WA 98195-3925, USA.
[3]Mechanical Engineering Department, University of Washington
3900 E Stevens Way NE, Box 352600
Seattle, WA 98195-2120, USA.

ABSTRACT

The interaction between a tool and part during composites manufacturing may significantly contribute to the formation of residual stresses and process-induced deformations (PIDs). Aerospace manufacturers typically treat tool surfaces with release coatings to minimize tool-part interaction. During autoclave processing, tool surfaces undergo physicochemical changes due to the aging of release coating and cure-induced contamination. The aging of release coating and surface contamination may strongly influence the level of tool-part interaction and PIDs in subsequent processing cycles. Production tools are frequently retreated with fresh layers of release coating and intermittently cleaned to mitigate aging and contamination effects. However, release coating reapplications and tool surface cleaning are often performed based on know-how in production environments, leading to cost-deficient tool preparation schedules, and in some cases excessive PIDs. This paper presents an automated method to evaluate the surface condition of large production tools for composites manufacturing using machine learning (ML) and sparse sensing. ML methods are used in conjunction with multiple measurement techniques for fast global digital mapping and sparse local physicochemical evaluation of a tool surface. The technology can be integrated into a robotic platform for automatic inspection of large tools to improve production efficiency and potentially mitigate PIDs in composites manufacturing.

Keywords: Composites Manufacturing, Tooling Inspection, Machine Learning
Corresponding author: Navid Zobeiry

1. INTRODUCTION

Aerospace composites manufacturing is a series of complex and interdependent processes that may lead to the formation of residual stresses in parts and, consequently, process-induced deformations (PIDs) [1-4]. Residual stresses develop during processing primarily due to a mismatch of free strains at the micro-, macro-, coupon-, and component-levels [1]. Other factors, however, may also significantly contribute to the formation of residual stresses and PIDs, including interfacial bonding and/or friction between a production tool and composite part (i.e., tool-part interaction) [5-13]. In the aerospace industry, production tools are typically prepared with release coatings prior to part lay-up to mitigate residual stress formation and PIDs induced by tool-part interaction. Release coatings also facilitate the removal of cured parts from tools after processing [14].

Aerospace manufacturers typically use a three-step process to prepare production tools such as Invar with release coatings. First, the tool is treated with solvent-based mold cleaner to remove any residue from previous processing/handling and create a clean mold surface (Fig. 1a). Depending on the severity and amount of resin residue on the tool surface, abrasive cleaning methods (e.g., coarse pads) or nonabrasive industrial methods (e.g., dry ice blasting) may be used in addition to solvent cleaning. However, abrasive methods may increase the tool surface roughness and consequently promote tool-part interaction, residual stresses, and PIDs. Next, a mold sealer is applied directly on the tool surface to fill micro-cavities, cover scratches, and prevent mechanical interlocking (i.e., physical bonding) between the tool and part (Fig. 1b). Then, several layers of release agent (RA) are applied on top of the sealed surface to form a low-energy barrier that prevents the formation of strong adhesive bonds and minimizes tool-part friction (Fig. 1c) [14]. Mold sealer and RA combine to form an abhesive and impenetrable release coating between the tool and part during lay-up and processing.

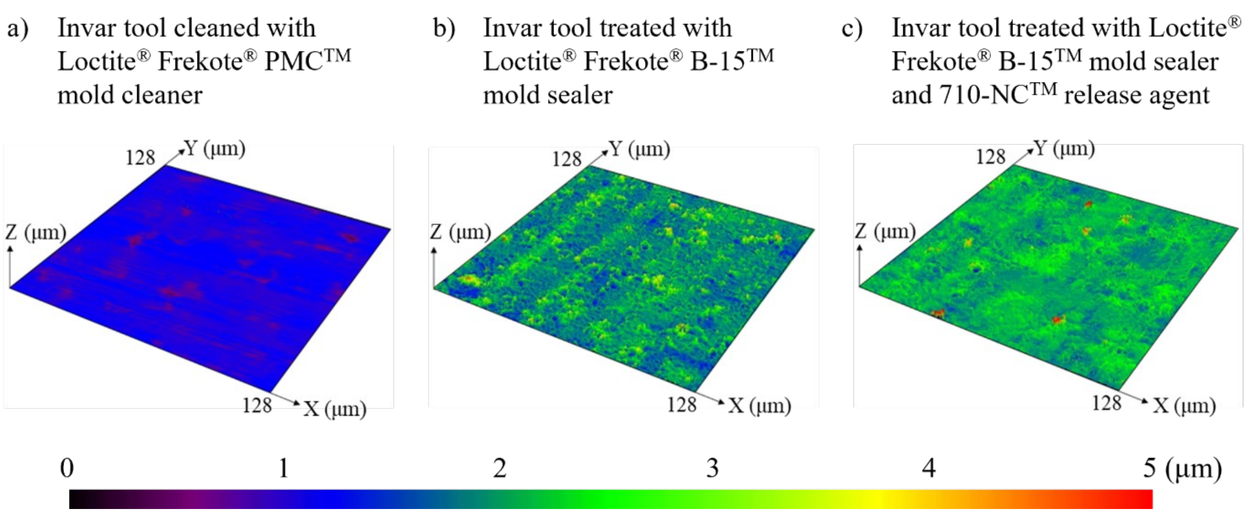

Figure 1. Standard steps of tool preparation in aerospace composites manufacturing: a) remove residue and create a clean tool surface with mold cleaner, b) cover surface pores and scratches with mold sealer, and c) minimize surface free energy with release agent. Images in this figure were collected using an Olympus LEXT OLS4100 laser scanning digital microscope.

The aerospace industry typically uses silicone-based release coatings due to their low adhesion (i.e., high abhesion) and high thermal/chemical stability properties. Silicone-based coatings are usually applied as liquids and cured through an evaporation reaction to form thin polymer barriers on the tool surface. During the cross-linking reaction of thermoset composites, some release coating molecules transfer from the tool to the part's surface and become physically and chemically integrated into its resin network. The transfer of molecules decreases the thickness of the remaining coating layer on the tool surface [15]. Elevated temperatures and pressures during autoclave processing may also cause resin to bleed from the prepreg, stick into surface cavities, and contaminate the tool. Consequently, each successive processing cycle results in a further reduction of coating thickness, an increase in its contamination level, and thus, a decrease in overall abhesion properties. The resultant change in physical and chemical properties due to processing can be considered the “aging” of release coating. The aging of release coating may strongly influence the level of tool-part interaction, residual stresses, and PIDs in subsequent processing cycles.

Standard practice within the aerospace industry to mitigate aging and maintain effective tool abhesion is to frequently reapply fresh layers of RA on top of the aged coating in between processing cycles. Mold sealers are seldom reapplied on top of aged coats due to their inherently long cure times, but RAs can typically be reapplied and cured relatively quickly. In production environments, RA reapplications and tool surface cleaning schedules are often based on tacit and know-how knowledge. This often leads to process specifications containing a high frequency of RA reapplications to ensure the successful demolding of parts. In addition to cost considerations and reducing production rate, overapplying RA layers may affect the final bonding quality of parts [15,16]. Conversely, too few reapplications could lead to costly problems such as excessive PIDs or non-demoldable parts after processing. Another approach that may be used to mitigate aging effects is to completely clean the tool using a combination of solvents and dry-ice blasting, then retreating it with fresh layers of mold sealer and RA. However, this latter method is particularly disruptive to the flow of manufacturing and is therefore only used when tools are highly contaminated and need thorough cleaning.

Aerospace manufacturers lack an automated non-destructive inspection method to evaluate tool surface condition and release coating during composites manufacturing. This is partly due to the requirement of utilizing portable analysis equipment for in-production tool inspections. Unfortunately, measurements gained from portable equipment often suffer in precision compared to results obtained from scientific-grade laboratory instruments due to differences in sampling methods, resolution, and overall equipment capabilities [17]. This lack of precision in portable analysis equipment may result in false-positive or false-negative tool surface evaluation, and thus offer insignificant improvements over manual inspection methods. Fortunately, powerful statistical tools such as machine learning (ML) and data-driven modeling may be used to enhance the quality of low-fidelity results by connecting them to high-precision laboratory measurements.

This paper presents a novel ML-based inspection method for in-production evaluation of tool surface condition and release coating during composites manufacturing. The technique utilizes ML and data-driven modeling in conjunction with digital imaging, contact angle goniometry, and Fourier-transform infrared spectroscopy (FTIR) to provide fast global mapping and sparse local physicochemical evaluation of a tool surface. Furthermore, ML methods are utilized to extract and analyze scientific-grade information from convenient but relatively low-quality portable measurements. The technology is intended to be integrated into a robotic platform for automatic inspection of large aerospace production tools. The novel method can be applied to reduce untimely RA reapplications, improve the efficiency of tool preparation, and potentially mitigate PIDs in aerospace composites manufacturing.

2. EXPERIMENTATION

2.1 Materials

The release coating used in this study consisted of two gold-standard aerospace products: Loctite® Frekote® B-15™ mold sealer and 710-NC™ release agent. The exact formulations of Frekote products are proprietary, but basic information is listed on publicly available datasheets [18,19]. The composition by weight of Frekote B-15 mold sealer includes 1-5% silicone components (reaction product of TMAS and PDMS) and 90-100% dibutyl ether as the solvent. The composition by weight of Frekote 710-NC release agent includes 1-5% silicone components (reaction product of TMAS and PDMS), 1-5% octane, 1-5% hydrocarbons (C7-10), 60-100% petroleum as the carrier, and 10-30% dibutyl ether as the solvent. Polydimethylsiloxane (PDMS) acts as the active silicone in both Frekote mold sealer and release agent, which allows for chemical compatibility between the two products, high abhesion (i.e., low surface free energy), and high chemical/thermal stability [14]. After the release coating components are applied on tools, most of the carrier and solvent evaporate, while the silicones and hydrocarbons remain and form micro-agglomerations on the lay-up surface (Fig. 1b,c).

The composite material used in this study was Toray T800S/3900-2 UD prepreg with a resin content of 35 % by weight [20]. 3900-2 is a toughened aerospace-grade epoxy resin, while T800S is an intermediate modulus and high strength carbon fiber. In addition to epoxy resin, the prepreg's surface is partially covered with micro-spherical thermoplastic tougheners. In recent decades, the T800/3900-2 system has been used as a primary structural material on major aircraft such as Boeing 787.

2.2 Method

The experimental method consisted of sequential rounds of tool preparation, autoclave processing, and tool inspection. First, two production tools were prepared to have identical surface conditions with equivalent amounts of release coating. These tools were then used as mold surfaces throughout twenty autoclave processing cycles of composite parts. Throughout the processing campaign, one tool was treated with one fresh layer of RA after every three cycles, while no RA reapplications were conducted on the other tool. This approach was used to investigate the effects of RA reapplications on aging. Then, after a pre-determined number of autoclave processing cycles, a novel technique was used to inspect the surfaces of both tools. Tool inspections were performed after each autoclave cycle for the first five cycles, then after every five cycles through the remainder of the campaign. Each inspection session consisted of using portable analysis equipment to identify signs of aging and contamination on the production tool surfaces. The experimental campaign continued until significant aging and contamination on the tool surface caused evident declines in tool abhesion properties. The overall goal of the procedure was to develop and validate the novel inspection technology's ability to identify and evaluate process-induced aging of release coating and contamination in a production environment.

In addition to using portable devices to evaluate production tools, each inspection step consisted of utilizing laboratory instruments to analyze small-scale test coupons. Coupons were initially prepared to mimic each surface condition on both production tools, then underwent RA reapplications and autoclave processing cycles in a parallel manner. One-half of the coupons were analyzed using FTIR, and the others were used for contact angle testing. The portability of the coupons allowed for high-precision laboratory analysis of each surface condition, which would later be used as a reference to enhance the low-fidelity portable measurements through ML techniques. Data analysis and ML methods were conducted using various libraries within Python and MATLAB.

2.3 Sample Preparation

Two Invar plates with approximate dimensions of 3 mm (t) × 300 mm (w) × 600 mm (l) were used as production tools. Twelve Invar coupons were made by cutting 25 mm (w) × 25 mm (l) square sections from a 0.25 mm (t) Invar sheet. Approximately three-fourths of each production tool was used as a lay-up surface, while the other one-fourth was used to support coupons during processing. Production tool and coupon surfaces were prepared using the following procedure:

Step 1: Both production tools and all twelve coupons were cleaned with Loctite® Frekote® PMC™ mold cleaner to remove any surface residue from previous cutting or handling.

Step 2: Two layers of B-15 mold sealer were applied to the lay-up surfaces of each production tool and coupon using a lint-free cotton wiping cloth, allowing 30 minutes between coats and after the final coat. Then, the production tools and coupons were placed in a convection oven for 60 minutes at 95 °C to accelerate the curing process as recommended on the product’s datasheet [18].

Step 3: The lay-up area of each production tool was divided into three geometrically-equivalent sections. The sections were prepared with either one, three, or five layers of RA. A lint-free cotton wiping cloth was used to apply RA layers, allowing 15 minutes between coats. The coupons were similarly prepared with either one, three, or five layers of RA using the same technique. Four coupons were treated with one layer, four were treated with three layers, and the other four were treated with five layers of RA. Two coupons with each surface condition (i.e., one, three, five layers of RA) were adhered to each production tool’s unsealed section using flashbreaker tape.

Step 4: One ply of T800S/3900-2 UD prepreg with nominal dimensions of 250 mm (w) × 400 mm (l) was laid-up to cover the release-coated areas on each production tool surface. Then, one 20 mm (w) × 20 mm (l) ply of UD prepreg was laid-up on each coupon.

Step 5: Each production tool and set of coupons was covered with one sheet of fluorinated ethylene propylene (FEP) release film, followed by one layer of breather cloth. The tools and lay-ups were placed and sealed in separate vacuum envelope bags (produced by Torr Technologies, Inc.), loaded into an autoclave, and subjected to the Manufacturer’s Recommended Cure Cycle (MRCC) [20]. The temperature cycle consisted of heating to 180 °C at 2 °C/min, holding at 180 °C for 120 minutes, then cooling the system down. A pressure of 0.7 MPa (7 atm.) was applied throughout processing.

Step 6: Once the cure cycle was complete, the envelope bags were removed from the autoclave and all composite parts were demolded from the tools and coupons. Test coupons were removed from the production tools and stored in sealed bags until the next processing cycle or inspection.

Step 7: Steps 4-6 were repeated before each round of inspection for a total of twenty rounds. One of the production tools and set of coupons were treated with one fresh layer of RA every three cycles. The other tool and coupons underwent all twenty rounds of autoclave processing without receiving any RA reapplications.

2.4 Tool Inspection Technology

Fig. 2 shows the novel system used to evaluate the surface condition of production tools throughout the testing campaign. The inspection set-up consisted of three compact devices: a Thorlabs Zelux® 1.6 MP Color CMOS Camera, a Jiusion USB Digital Microscope, and an Agilent 4100 ExoScan Handheld FTIR. Each instrument was integrated into a mechanical gantry system, which allowed for three-dimensional portability over the entire tool surface area. The portable devices were used in conjunction with ML and data-driven modeling techniques to form a three-step inspection procedure: global mapping, sparse surface free energy (SFE) evaluation, and sparse chemistry evaluation.

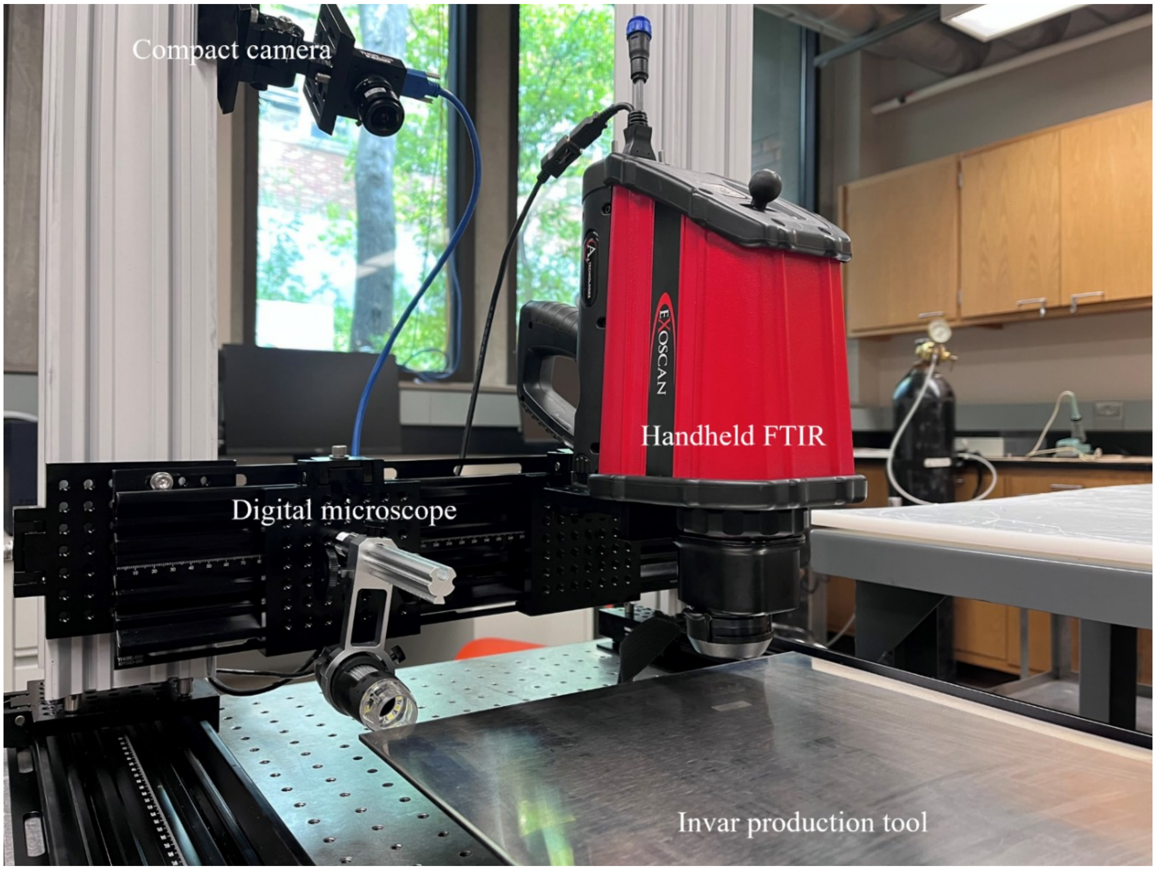

Figure 2. Novel inspection technology for tool surface evaluation in composites manufacturing. The set-up consists of three portable analysis devices (i.e., compact camera, digital microscope, and handheld FTIR) mounted onto a mechanical gantry system.

2.4.1 Global Mapping

The first step of the inspection process was to collect a top-down RGB image of the tool surface using the compact camera. The camera was mounted at a fixed position, allowing it to capture the entire tool surface in one shot (i.e., global mapping). Each image was then analyzed using a novel ML-based filtering system that was trained using supervised learning to identify areas on a tool surface containing color abnormalities. The pixels within and surrounding color-abnormal regions were then classified into three categories: abhesive release coating, aged release coating, and contamination. Classifications were assigned based on each pixel's single-channel color value. The spatial coordinates of the identified color-abnormal region were then used as a target area for sparse evaluations in the following two inspection steps.

2.4.2 Sparse Surface Free Energy Evaluation

The next inspection step was evaluating SFE throughout the target area. SFE measurements were conducted using the digital microscope on production tools in conjunction with a high-precision laboratory instrument on coupons. Calculations of SFE require contact angle analysis of two different liquids on a solid surface – one liquid being dominantly polar and the other primarily dispersive. Unfortunately, measuring contact angles of many dispersive liquids presents challenges due to their inherently high sensitivities to drop size [21]. The portable inspection set-up utilized a manual dispensing system, which was only sufficient for analyzing the polar component. Laboratory equipment was used for the dispersive liquid that required a highly-controlled dispensing system. Di-ionized (DI) water and diiodomethane (DIM) were used as the polar and dispersive liquids, respectively.

During portable inspection, a total of 150 DI water droplets with approximate volumes of 50 µL were manually dispensed within the target area using a pipette. The number of droplets was equally divided between each surface condition classified during global imaging – 50 on abhesive release coating, 50 on aged release coating, and 50 droplets on resin contamination. The digital microscope was used to collect side-view images of each droplet immediately after solid-liquid contact on the tool surface. The contact angle and width-to-height aspect ratio of each droplet were then calculated using ImageJ processing software. An AST video contact angle system was used to collect laboratory measurements of five DIM contact angles on each surface condition. Due to a lack of aged release coating spots on small coupons, an uncoated Invar tool was used as the solid substrate to represent the aged surface condition during laboratory analysis. The average of the five angles was then used in conjunction with each DI water contact angle to calculate SFEs using the Owens-Wendt method [22]. The dispersive and polar tensions of DI water were assumed to be 22.1 dyne/cm and 50.7 dyne/cm, respectively. The dispersive and polar tensions of DIM were assumed to be 48.5 dyne/cm and 2.3 dyne/cm, respectively.

2.4.3 Sparse Surface Chemistry Evaluation

The third inspection step was evaluating surface chemistry throughout the target area. Similar to SFE evaluations, chemistry measurements were conducted using portable and laboratory analysis equipment (i.e., FTIR spectrometers) on production tools and coupons, respectively. However, the aged surface condition was analyzed using only portable equipment due to the lack of aged release coating spots on small coupons. The handheld FTIR was used for portable analysis on the basis of diffuse reflectance, while a Bruker Vertex 70 FTIR Spectrometer was utilized on the basis of attenuated total reflectance (ATR) for laboratory measurements. Three IR-absorbance spectra were scanned on each surface condition classified during global imaging in a spectral range of 500-4000 cm^{-1}. The three spectra were normalized, averaged, and plotted for analysis.

3. RESULTS

As previously mentioned, tool inspections were conducted after each autoclave cycle for the first five cycles, then after every five for a total of twenty cycles. Throughout the twenty-cycle campaign, both production tool surfaces underwent significant chemical changes, but remained highly abhesive for nineteen of the twenty processing cycles. Upon demolding after the twentieth cycle, the production tool which received no RA reapplications showed significant aging effects. These effects caused an evident reduction in tool abhesion, resulting in a large required force to demold the composite part. Conversely, the tool subjected to periodic RA reapplications showed no aging effects after twenty rounds of autoclave processing. These results indicate that reapplying one RA layer after every three processing cycles mitigates release coating aging effects. The remainder of this section focuses on the tool that received no RA reapplications and thus exhibited significant aging after twenty processing cycles. The results reported in this section are meant to demonstrate the novel inspection technology's potential to identify and evaluate aged release coating and contamination in a production environment.

3.1 Global Mapping

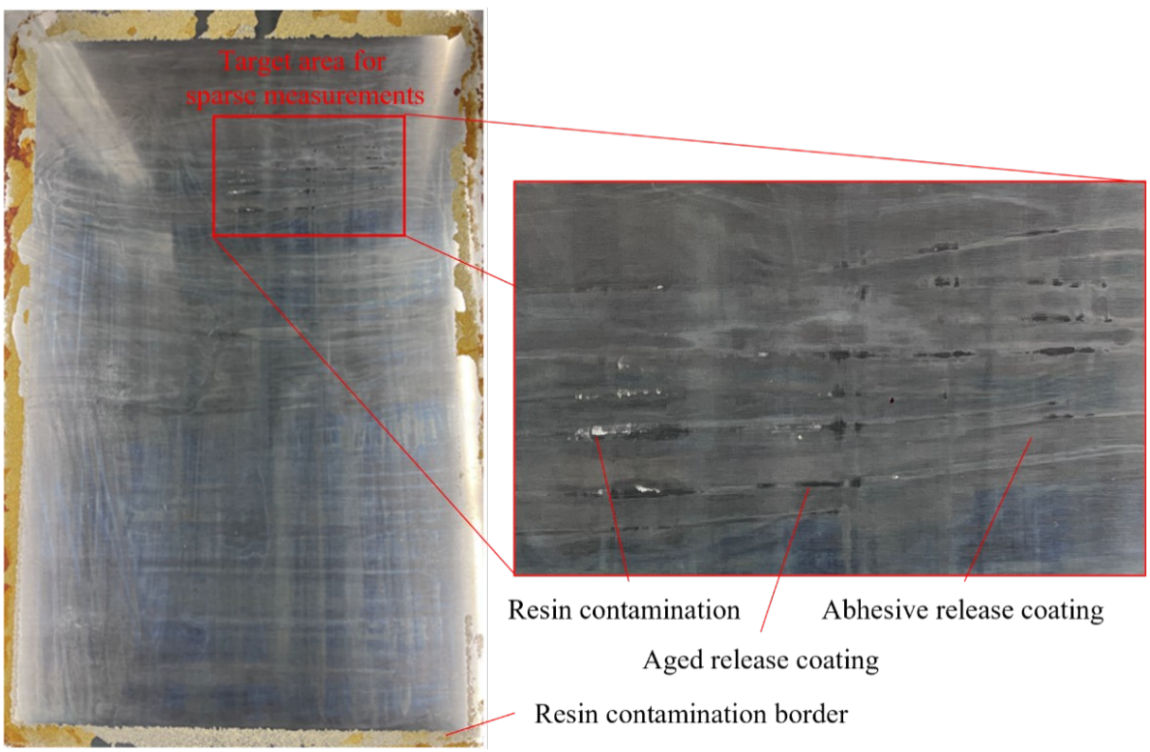

Figure 3. Image of tool surface after undergoing twenty autoclave processing cycles without any RA reapplications. Most of the tool surface is covered with abhesive release coating (opaque), but also contains patches of resin contamination (light) and aged release coating (dark).

Fig. 3 shows an image of the production tool surface after undergoing twenty autoclave processing cycles without any RA reapplications. The image demonstrates that elevated temperatures and pressures during processing caused resin to bleed from the prepreg, flow to the tool's outside edges, and cure to the surface as a contamination border. The thickness and surface area of resin contamination increased with each processing cycle and consequently decreased the area of abhesive release coating on the tool surface. If production tools are not cleaned regularly, contamination can continue to grow into the lay-up surface and have detrimental effects on tool abhesion, PIDs, and end-part quality. Throughout the twenty autoclave processing cycles, the contamination border remained outside the lay-up dimensions of the composite parts. Therefore, the significant decrease in tool abhesion after twenty cycles was likely due to aging within the lay-up boundaries rather than from the contamination border. The remainder of the inspection was thus conducted within the tool's lay-up boundaries.

The red box in Fig. 3 outlines the target area identified by the supervised ML model to contain color abnormalities. After twenty processing cycles, the tool's lay-up surface was mainly covered by an opaque, abhesive release coating. However, the tool section that was initially treated with only one layer of RA contained light and dark patches on its surface. Light patches corresponded to resin contamination, while dark patches were aged release coating (verified using handheld FTIR). A lack of contamination and aging in other sections indicates that applying more RA layers prior to processing creates a longer-lasting barrier between the tool and part. In other words, the number of RA layers may directly affect the rate of aging on a tool surface. Nevertheless, all of the significant aged and contamination patches were contained in the target area, demonstrating the ML model's ability to effectively identify color defects on a tool surface.

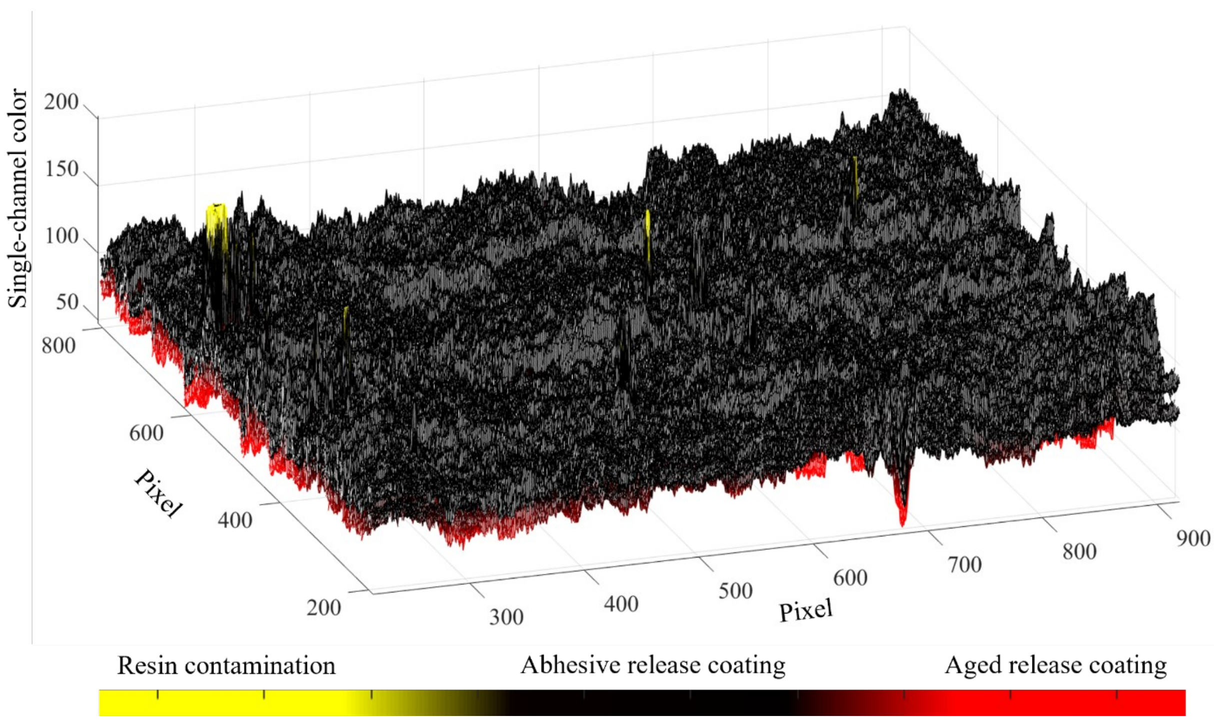

Figure 4. Surface plot of target area containing color abnormalities. A supervised ML filter was applied to the plot to classify pixels as either resin contamination (yellow), abhesive release coating (black), or aged release coating (red) based on single-channel color values.

Fig. 4 shows a portion of the target area plotted as a three-dimensional surface after being subjected to ML filtering. The ML filter classified pixels in the plot into three categories: resin contamination (yellow), abhesive release coating (black), or aged release coating (red). The plot's x- and y-axes correspond to coordinates in the target area in units of pixels, while the z-axis represents each pixel's single-channel color value. In addition to providing a visual of the target zone, a plot similar to Fig. 4 may be utilized in a production environment to quantify the spatial coordinates, distribution, and percent area of aged release coating or resin contamination on a tool surface. During an inspection, these values could then be used as go/no-go (i.e., pass/fail) criteria.

3.2 Sparse Surface Free Energy Evaluation

Fig. 5 shows side-view images of DI water droplets immediately after solid-liquid contact with a) abhesive release coating, b) aged release coating, and c) resin contamination within the tool's target area. The images in the figure were captured using the low-fidelity portable digital microscope. The top half of each image shows the droplet resting on various tool surface conditions, while the bottom half shows the droplet's reflection in the Invar tool. When dispensed on the three different surface conditions, DI water droplets formed unique contact angles and distinct spherical shapes. Droplets applied to abhesive release coating exhibited the largest contact angles and lowest width-to-height aspect ratios (i.e., spreading). Conversely, droplets dispensed on resin contamination yielded the lowest contact angles and highest aspect ratios. The contact angle and shape a liquid droplet makes on a solid surface directly results from intermolecular adhesive interactions at the solid-liquid interface due to SFE effects and internal cohesive forces in the liquid [21]. Since liquid properties of DI water remained constant throughout the inspection procedure, each droplet's unique contact angle and shape must have been due to SFE effects. Therefore, even without performing robust calculations, the portable technique was able to identify distinct qualitative differences in SFE between abhesive release coating, aged release coating, and resin contamination.

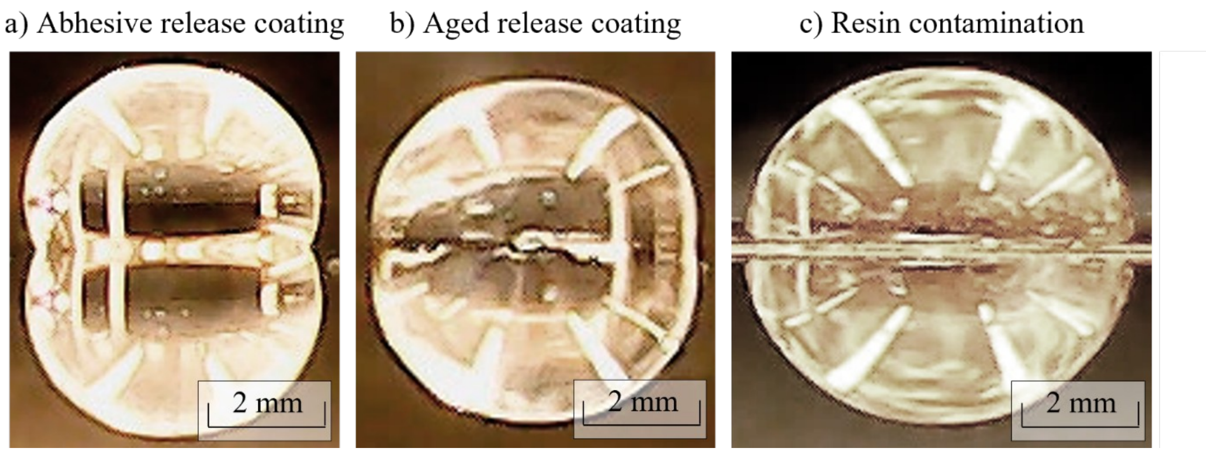

Figure 5. DI water droplets immediately after solid-liquid contact with a) abhesive release coating, b) aged release coating, and c) resin contamination on a tool surface.

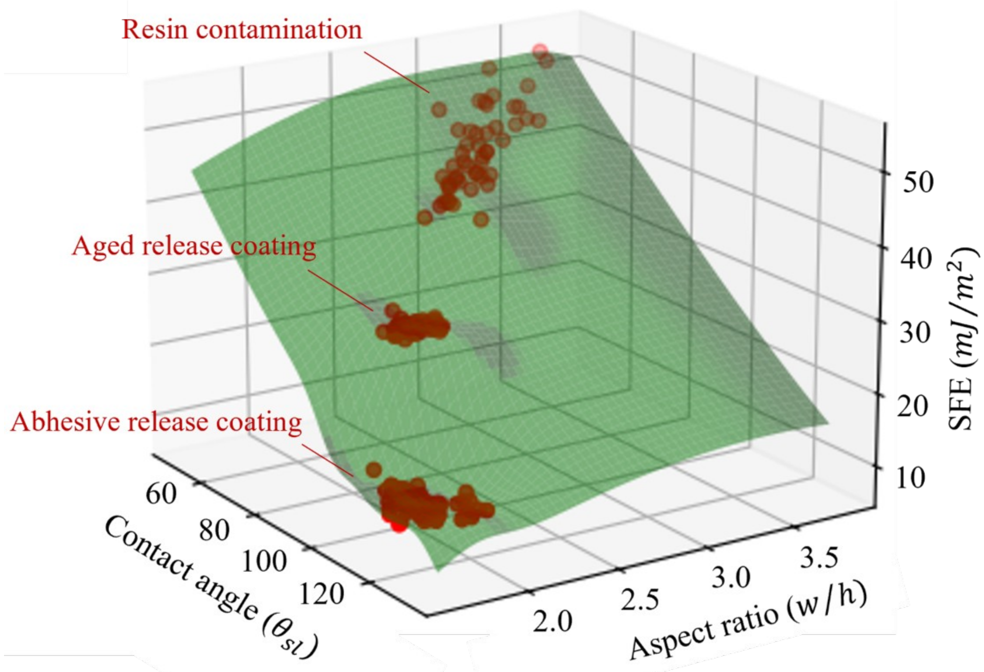

Figure 6. Surface free energy (SFE) versus contact angle and aspect ratio of DI water droplets on abhesive release coating, aged release coating, and resin contamination.

Fig. 6 shows a plot of SFE versus DI water contact angle and aspect ratio, with red points representing calculated or measured values. A response surface, shown in green, was fitted to the data using a supervised ML method, Gaussian Process Regression (GPR). GPR models possess several benefits, one of which includes working well on small datasets, such as the one represented in Fig. 6. The SFEs of abhesive release coating areas were measured over an approximate range of 11-13 mJ/m^2. These exceptionally low values indicate the majority of the target area and tool surface remained highly abhesive after undergoing twenty processing cycles without any RA reapplications. Aged release coating and resin contamination SFEs were measured over approximate ranges of 28-30 mJ/m^2 and 38-53 mJ/m^2, respectively. Surface patches containing these higher SFE values were likely the cause of decreased tool abhesion properties after the twentieth autoclave cycle. Furthermore, the largest SFE values measured on resin indicates that contamination has more detrimental effects on tool-part interaction and PIDs than aged release coating. The standard deviations (SDs) of abhesive, aged, and contaminated areas were approximately 0.4 mJ/m^2, 0.2 mJ/m^2, and 3.5 mJ/m^2, respectively. The notably larger scatter in contamination measurements was likely due to a combination of uncontrolled DI water dispensing and the non-uniform macro-roughness of cured resin [21,23].

The model in Fig. 6 may be utilized as a quick method to classify surface conditions or predict tool SFEs for inspection criteria. For example, if high values of SFE (e.g., 30-50 mJ/m^2) are measured, the tool should be cleaned before further processing. On the other hand, if intermediate SFE values are predicted using the GPR model (e.g., 15-25 mJ/m^2), further investigation of the tool surface may be necessary.

3.3 Sparse Surface Chemistry Evaluation

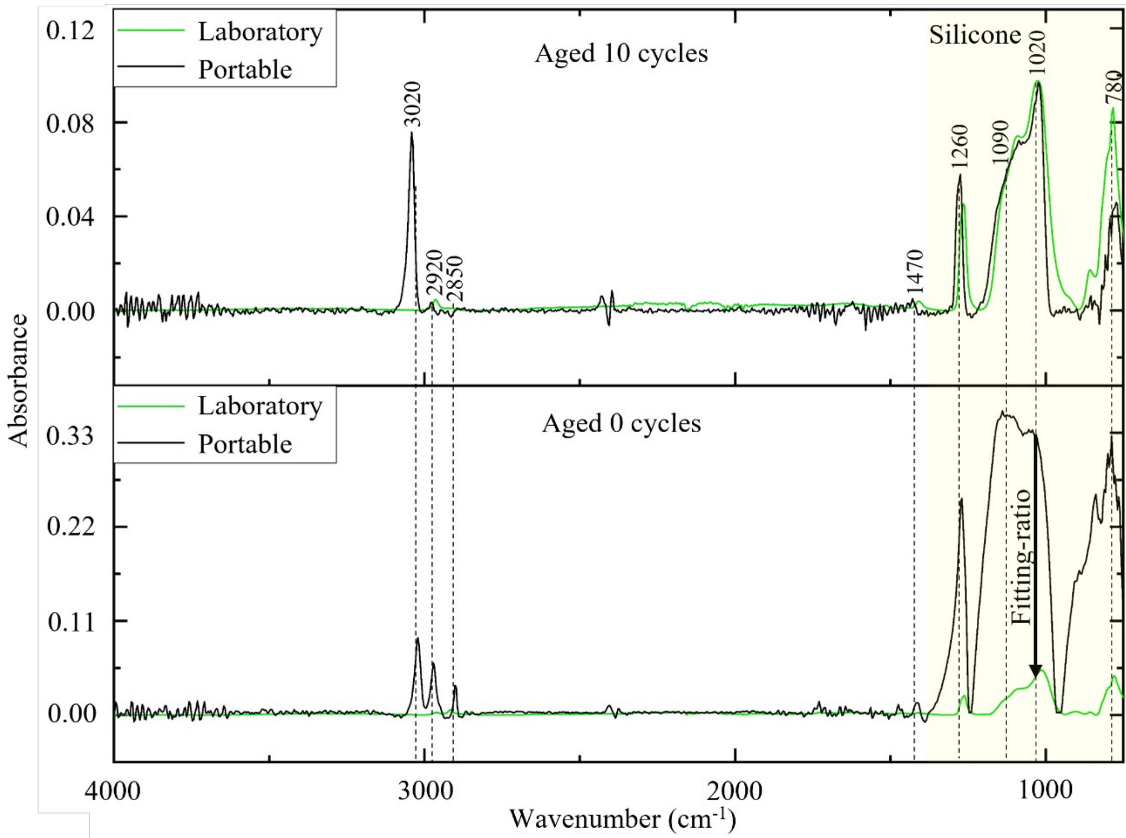

Figure 7. IR-absorbance spectra of fresh and aged release coating. A fitting ratio must be calculated to transform results obtained using portable equipment prior to tool conditioning into laboratory-quality measurements.

Fig. 7 compares IR-absorbance spectra of fresh (i.e., aged 0 cycles) release coating with release coating that underwent ten autoclave processing cycles. The portable spectra in the plots were taken within the tool's target area, while laboratory spectra were measured on coupons. Fig. 7 is meant to illustrate how fresh and aged release coating exhibit different chemical characteristics, and how portable analysis results may differ from measurements obtained through laboratory instruments. Fresh and aged release coating exhibit similar general peaks at wavenumbers of 3020, 2920, 2850, 1470, 1260, 1090, 1020, and 780 cm^{-1}. The four peaks at 780, 1020, 1090, and 1260 cm^{-1} are characteristic of silicone materials – specifically a PDMS polymer network [14,15,17]. The peak at 780 cm^{-1} represents Si-CH_3 bond stretching. The peaks at 1020 and 1090 cm^{-1} represent the asymmetric stretching of Si-O-Si bonds. The peak at 1260 cm^{-1} is characteristic of the symmetrical deformation of the C-H bond in the Si-$(CH_3)_2$ groups (i.e., Si-CH_3 bending). There also exists a weaker peak at 1470 cm^{-1} and a strong cluster around 3020 cm^{-1}, which represent C-H scissoring and asymmetric C-H stretching, respectively.

Although the fresh and aged spectra contain IR-peaks at similar wavenumbers, Fig. 7 also demonstrates chemical differences between the two surface conditions. For example, according to laboratory measurements, all of the peaks within the silicone regime underwent an approximate two-fold intensity increase during the first ten autoclave cycles. These chemical changes were likely due to the tool becoming “conditioned” to the release coating, which is a consequence of using a new and freshly coated tool. During a production tool’s first few processing cycles, external temperatures and pressures cause non-silicone components to flash off or transfer to the part, while silicone components are “baked” into the mold [19]. These conditioning mechanisms cause variations in the release coating’s chemical composition (i.e., silicone levels), which are captured in the laboratory IR-absorbance spectra of Fig. 7. After the tool becomes conditioned, the properties of release coating are considered “locked-in” and remain stable until considerable aging effects cause silicone levels and tool abhesion to drop.

As previously mentioned, measurements gained from portable equipment often suffer in precision compared to results obtained from scientific-grade laboratory instruments due to differences in sampling methods and overall equipment capabilities. This lack of precision is demonstrated by significant mismatches between portable and laboratory spectra in Fig. 7. For fresh release coating, all silicone peaks in the portable spectrum are approximately five times larger than the precise laboratory measurements. In a production environment, an inaccurate measurement such as this could result in false-positive or false-negative tool surface evaluation. Fortunately, the portable silicone regime becomes similar to laboratory measurements once the tool becomes conditioned and properties are locked-in. These results suggest that portable FTIR equipment may be faulty prior to tool conditioning, but is more reliable after silicone levels stabilize.

Fig. 8 shows a plot of 1020 cm^{-1} absorbance peak intensity versus the number of RA layers and processing cycles (i.e., age of release coating). Red points in the plot were measured throughout the testing campaign in different areas on the production tool using the portable FTIR. A response surface, shown in green, was fitted to the data using GPR with an accuracy of 86%. The blue surface in the plot represents the general behavior of laboratory measurements throughout the campaign and is meant to be used as a qualitative comparison with portable results. The 1020 cm^{-1} peak was chosen for the model to quantify silicone levels on the tool surface as a function of RA layers and processing cycles. The portable and laboratory response surfaces show large differences over the first five autoclave cycles for all surface conditions due to the tool becoming conditioned to release coating. Measuring an unusually high 1020 cm^{-1} absorbance in a production environment could be an indication of an unconditioned tool. Collecting accurate information from portable equipment prior to conditioning requires calculating a fitting-ratio by dividing the laboratory peak intensity by its portable counterpart. However, calculating a fitting-ratio requires the tool surface history to be known, including the number of RA layers and processing cycles.

After reaching the five-cycle mark, the portable and laboratory absorbances plateaued and remained relatively constant through the remainder of the testing campaign. The portable response surface remained within approximately 10% of laboratory results between the fifth and twentieth cycles. This consistent accuracy demonstrates the portable equipment’s ability to evaluate the surface chemistry of release coating after conditioning occurs. Hence, portable results do not have to be connected to laboratory measurements for accurate characterization of release coating. Using a fitting-ratio after conditioning occurs would still increase the fidelity of portable measurements, but may not be essential during inspections. Portable FTIR results from one of the aged patches in the tool’s target area are also shown in Fig. 8. The aged patch contained a near-zero 1020 cm^{-1} absorbance, indicating a lack of silicone in that region. These effects validate the ability of portable FTIR to identify sufficiently aged release coating on a tool surface.

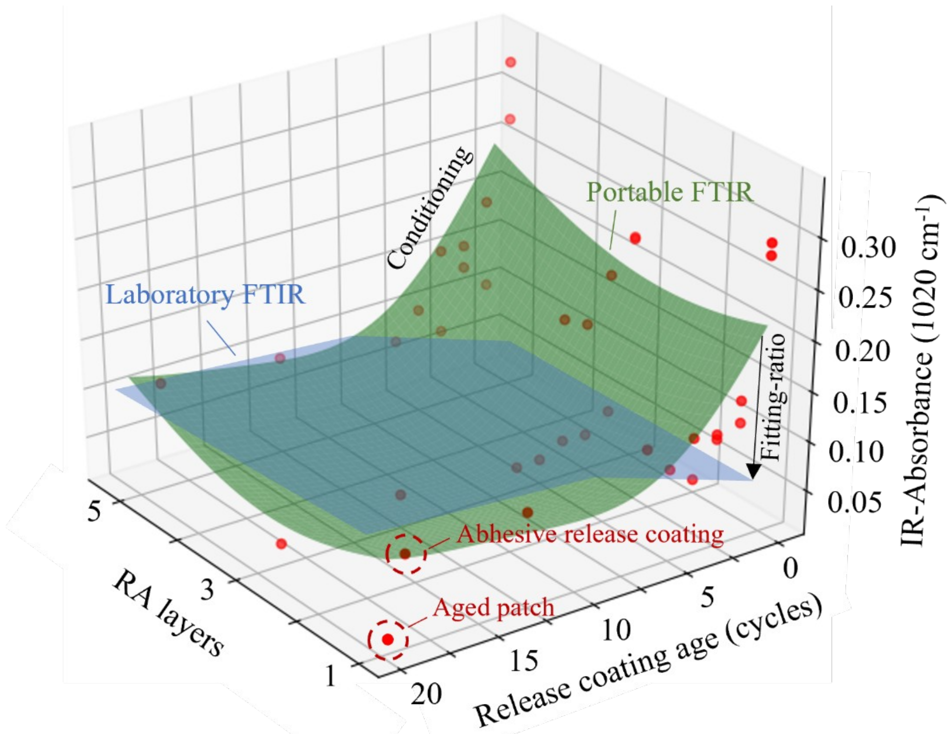

Figure 8. GPR model of 1020 cm^{-1} silicone absorbance peak intensity in Frekote release coating versus the number of RA layers and processing cycles. The model can be used to predict surface history or silicone composition on a production tool using portable FTIR measurements.

4. CONCLUSIONS

The objective of this study was to develop a non-destructive and portable method for in-production evaluation of tool surface condition during composites manufacturing. A novel technology was developed to achieve this goal by integrating portable analysis equipment into a mechanical gantry system. Each portable device was used in conjunction with ML and data-driven modeling techniques to form a three-step automated inspection procedure of tool surfaces. The main conclusions from this work are as follows:

- Treating a tool with two layers of Frekote mold sealer and several layers of release agent prior to processing creates a low-energy release coating. During processing, release coatings undergo significant chemical changes, but may remain highly abhesive for more than twenty autoclave processing cycles. The number of release agent layers applied to a tool impacts the coating’s effective lifespan. Periodic reapplications of release agent can be used to mitigate aging effects and maintain effective tool abhesion. However, frequent reapplications are unnecessary and may only disrupt the flow of manufacturing.

- Machine learning is an effective tool for increasing the fidelity of portable analysis equipment. Digital imaging can be used to evaluate large production tools and identify color abnormalities on a tool surface. Contact angle goniometry is a fast method for measuring surface free energy or identifying aged release coating and contamination. FTIR can be used to determine an approximate age of release coating and detect contamination.

Handheld FTIR devices may not be able to accurately evaluate release coating until after a tool surface becomes conditioned.

5. ACKNOWLEDGEMENTS

The work reported here was funded by the Joint Center for Aerospace Technology Innovation (JCATI) and Toray Industries, Inc. The authors would also like to acknowledge Henkel Aerospace for their generous donations of release coating products and The Boeing Company for their continued support. Part of this work was conducted at the Washington Clean Energy Testbeds, a facility operated by the University of Washington Clean Energy Institute.

6. REFERENCES

1. Zobeiry, N. and Poursartip, A. “3 - The origins of residual stress and its evaluation in composite materials.” *Structural Integrity and Durability of Advanced Composites*. Eds. Beaumont, P.W.R., Soutis, C., and Hodzic, A. Sawston, United Kingdom: Woodhead Publishing, 2015. doi: 10.1016/B978- 0-08-100137-0.00003-1.
2. Zobeiry, N., Forghani, A., Li, C., Gordnian, K., Thorpe, R., Vaziri, R., Fernlund, G., and Poursartip, A. “Multiscale characterization and representation of composite materials during processing.” *Phil. Trans. R. Soc. A*, 374 (2071) (2016): 20150278. doi: 10.1098/rsta.2015.0278.
3. Fernlund G., Mobuchon, C., and Zobeiry, N. 2018. “2.3 Autoclave Processing.” *Comprehensive Composite Materials II*. Eds. Beaumont, P.W.R. and Zweben, C.H. Oxford, United Kingdom: Academic Press, 2018: 42-62. doi: 10.1016/B978-0-12-803581-8.09899-4.
4. Li, C., Zobeiry, N., Keil, K., Chatterjee, S., and Poursartip, A. “Advances in the characterization of residual stress in composite structures.” *SAMPE Technical Conference Proceedings*. Seattle, WA, June 2-4, 2014. Society for the Advancement of Material and Process Engineering.
5. Twigg, G., Poursartip, A., and Fernlund, G. “Tool–part interaction in composites processing. Part I: experimental investigation and analytical model.” *Composites Part A: Applied Science and Manufacturing* 35(1) (2004): 121-133. doi: 10.1016/S1359-835X(03)00131-3.
6. Twigg, G., Poursartip, A., and Fernlund, G. “Tool–part interaction in composites processing. Part II: numerical modelling.” *Composites Part A: Applied Science and Manufacturing* 35(1) (2004): 135-141. doi: 10.1016/S1359-835X(03)00132-5.
7. Schoenholz, C., Slade, D., Zappino, E., Petrolo, M., Zobeiry, N. “Representation, Characterization, and Simulation of Tool-Part Interaction and Its Effects on Process-Induced Deformations in Composites.” *Proceedings of the 36th American Society for Composites Technical Conference*. College Station, Texas, September 20-22, 2021. Ed. Ochoa, O. DEStech Publications, Inc. 1204-1216. doi: 10.12783/asc36/35832.
8. Potter, K. D., Campbell, M., Langer, C., and Wisnom, M.R. “The generation of geometrical deformations due to tool/part interaction in the manufacture of composite components.” *Composites Part A: Applied Science and Manufacturing*. 36(2) (2005): 301-308. doi: 10.1016/j.compositesa.2004.06.002.

9. Twigg, G., Poursartip, A., and Fernlund, G. “An experimental method for quantifying tool–part shear interaction during composites processing.” *Composites Science and Technology* 63(13) (2003): 1985-2002. doi: 10.1016/S0266-3538(03)00172-6.

10. Ersoy, N., Potter, K., Wisnom, M.R., and Clegg, M.J. “An experimental method to study the frictional processes during composites manufacturing.” *Composites Part A: Applied Science and Manufacturing*. 36(11) (2005): 1536-1544. doi: 1016/j.compositesa.2005.02.010.

11. Zappino, E., Zobeiry, N., Petrolo, M., Vaziri, R., Carrera, E., and Poursartip, A. “Analysis of process-induced deformations and residual stresses in curved composite parts considering transverse shear stress and thickness stretching,” *Composite Structures* 241 (2020): 112057. doi: 10.1016/j.compstruct.2020.112057.

12. Kaushik, V. and Raghavan, J. “Experimental study of tool–part interaction during autoclave processing of thermoset polymer composite structures.” *Composites Part A: Applied Science and Manufacturing* 41(9) (2010): 1210–1218. doi: 10.1016/j.compositesa.2010.05.003.

13. Albert, C. and Fernlund, G. “Spring-in and warpage of angled composite laminates.” *Composites Science and Technology* 62(14) (2002): 1895–1912. doi: 10.1016/S0266-3538(02)00105-7.

14. Critchlow, G.W., Litchfield, R. E., Sutherland, I., Grandy, D.B., and Wilson, S. “A Review and Comparative Study of Release Coatings for Optimised Abhesion in Resin Transfer Moulding Applications.” *International Journal of Adhesion and Adhesives* 26(8) (2006): 577-599. doi: 10.1016/j.ijadhadh.2005.09.003

15. Blass, D., and Dilger, K. “CFRP-Part Quality as the Result of Release Agent Application – Demoldability, Contamination Level, Bondability.” *Procedia CIRP* 66 (2017): 33–38. doi: 10.1016/j.procir.2017.03.219.

16. Markatos, D.N., Tserpes, K.I., Rau, E., Markus, S., Ehrhart, B., and Pantelakis, Sp. “The effects of manufacturing-induced and in-service related bonding quality reduction on the mode-I fracture toughness of composite bonded joints for aeronautical use.” *Composites Part B: Engineering* 45(1) (2013): 556–564. doi: 10.1016/j.compositesb.2012.05.052.

17. Tracey, A., Flinn, B.D. “Infrared Spectroscopy: A Potential Quality Assurance Method for Composite Bonding Surface Preparation.” *Proceedings of the International SAMPE Technical Conference Series*. Baltimore, Maryland, May 21-24, 2012.

18. Henkel Corporation, “TDS Loctite® Frekote® B-15™,” Dec. 2013.

19. Henkel Corporation, “TDS Loctite® Frekote® 710-NC™,” Jan. 2015.

20. Toray Composite Materials America, Inc., “3900 PREPREG SYSTEM,” Jul. 2020.

21. de Gennes, P-G., Brochard-Wyart, F., Quere, D. *Capillarity and Wetting Phenomena*. New York, NY: Springer Publishing, 2004. doi: 10.1007/978-0-387-21656-0.

22. Owens, D.K., Wendt, R.C. “Estimation of the surface free energy of polymers.” *Journal of Applied Polymer Science* 13 (1969): 1741-1747. doi: 10.1002/app.1969.070130815.

23. Wenzel, R.N. “Surface Roughness and Contact Angle.” *The Journal of Physical and Colloid Chemistry* 53(9) (1949): 1466-1467. doi: 10.1021/j150474a015.